MEMS-based Magneto-Gyro sensor for Instrument Landing System (ILS) in Aircrafts

Suganya A[1], Duraiarasu E[2], Umesh S[3], Caroline Pushpa J[4]

[1]Phd scholar, Centre of Excellence in MEMS and Microfluidics, Rajalakshmi Engineering College, Thandalam, Chennai.
[2]UG Student, Department of Electronics and Communication Engineering, Rajalakshmi Engineering College, Thandalam, Chennai.
[3]UG Student, Department of Electrical and Electronics Engineering, Rajalakshmi Engineering College, Thandalam, Chennai.
[4]Research Assistant, Centre of Excellence in MEMS and Microfluidics, Rajalakshmi Engineering College, Thandalam, Chennai.
suganya.a.mems@rajalakshmi.edu.in

Abstract:

Magneto-Gyro sensor is a MEMS-based sensor where two Gyroscope and a Magnetometer is combined. The Magneto-Gyro Sensor is a device suggested for Instrument Landing Systems (ILS) in aircraft. A MEMS gyroscope and magnetometer are combined as a single device providing the attitude estimation and the heading of the system. Specifically for measuring the wing-to-wing attitude of the aircraft while landing along with the heading direction in an ILS. A resolution of 3 rads/sec has been achieved for the gyroscope.

***Keywords*: MEMS, Gyroscope, Magnetometer, ILS.**

I. INTRODUCTION

Instrument Landing System (ILS) provides the pilot of an aircraft with the vertical and horizontal positions of the vehicle while approaching landing. Though advanced landing systems have been developed they still lack lots of studies and improvements need to be made. ILS is considered as one of the best navigational aids in the history of aviation, with a few improvements like more sensitivity and a few safety requirements, ILS can still be used as a primary landing system in aircraft Suggesting an aid to the sensitivity of the system, we put forth a magnetometer and a gyroscope combined MEMS device.

A MEMS gyroscope provides the measurement of the angular rate of the system. A three-axis gyroscope has been suggested to measure the drift in all three axes providing a 3D orientation of the system in space. This angular rate measurement will help in the estimation of the system's attitude, which is very much useful in ILS. During the landing of the flights, stalling happens when the angle of attack exceeds the critical angle. To detect the wing-to-wing deviation from the initial axes, the use of the MEMS gyroscope is suggested. The MEMS magnetometer provides a measurement in the horizontal axis parallel to the earth's magnetic field taking the same as a reference. This can help in providing the heading of the system.

II. INNOVATION IN DESIGN

A. Novelty in design

The proposed sensor integrates the Gyroscope and Magnetometer together providing the novelty in our design.The Magneto-Gyro sensor is modelled in such a way to improve the resolution which makes the precision heading of the system.

B. Dimensional details

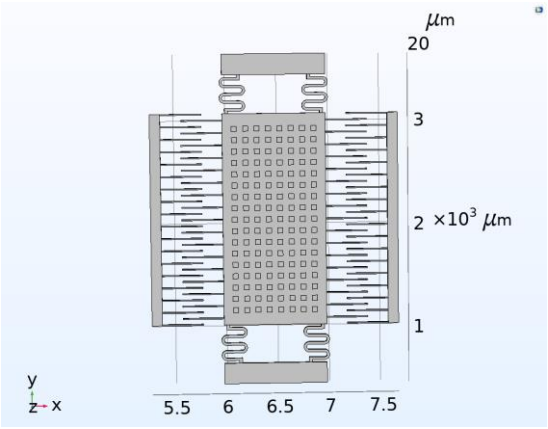

(a)

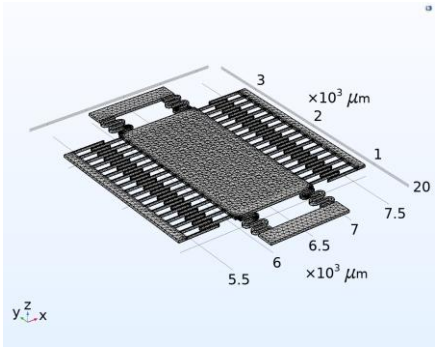

(b)

Fig 1: (a) Geometry and (b) mesh of the desired sensor

The centre part of the device is a magnetometer with gyroscope structures on either side. The overall size of the device is 2400µm×3200µm. The size of the perforations in the magnetometer is 50µm×50µm. Distance between two comb structures is 110µm. Thickness of a single comb is 10µm.

III. Theoretical Analysis and Simulation Results

We have simulated an integrated structure of a gyroscope and a magnetometer. The material chosen is a single crystal isotropic silicon because of its good mechanical and electrical properties. An AC current of 50mA is applied to the anchored terminal of the gyroscope and is grounded on the other side.

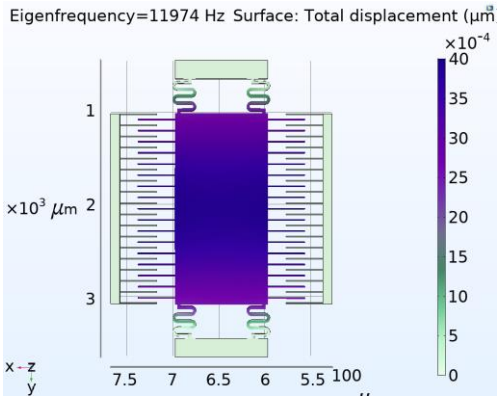

Fig 2: Maximum displacement at natural frequency.

Eigen frequency analysis of the magneto-gyro structure is shown in Fig 2. A constant current is supplied to the beam in the y-axis, simultaneously an external magnetic field is applied across the x-axis, and the resulting Lorentz force causes a deflection along the y-axis.

The Lorentz force generated is given by

$$F_L = I_e L B \qquad \text{..... [1]}$$

Where,

F_L is the generated Lorentz force

L is the length of the bar between the support arms

I_e is the applied current

B is the magnetic field

Fig 3 represents the maximum displacement of the magnetometer along the y-axis. Since the change is displacement is of the order of 10^{-20} which is negligible, this change will not affect the gyroscope's functioning, accounting for the stability of the structure.

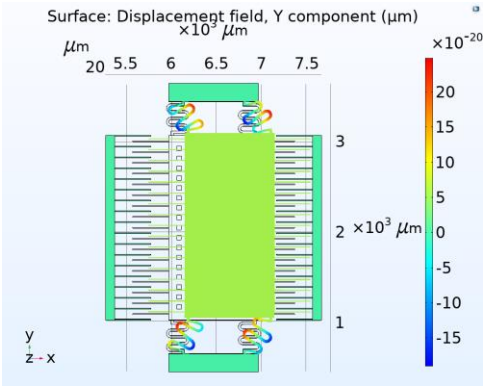

Fig 3: Displacement along z-axis for magnetometer

The angular velocity of the gyroscope is taken as the primary factor to denote the change in the gyroscope, which can be considered as the result of the Coriolis force. We apply force such that it works as a Rotational Centrifugal Force and the angular velocity is calculated from RPM (Rotations Per Minute) which is the result of RCF. RPM is calculated from the below formula.

$$RCF = (RPM)^2 \times 1.118 \times 10^{-5} \times R \qquad \text{..... [2]}$$

where, R is the radius of the rotating frame.

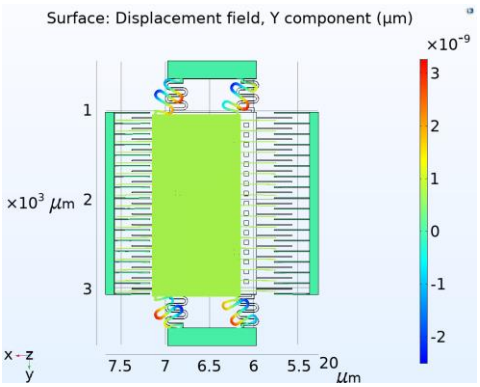

Fig 4: Displacement along z-axis for gyroscope.

Fig 4 represents the maximum displacement of the along the gyroscope y-axis. When an RPM of 1 rad/sec is applied in the rotating frame of the sensor there will be a change in rotating frequency, as a result of which the angular velocity changes. The change in angular velocity accounts for the change in displacement of the comb structure and this variation in displacement will account for the orientation and stability of the plane. Fig 5 provides the graphical analysis of the displacement.

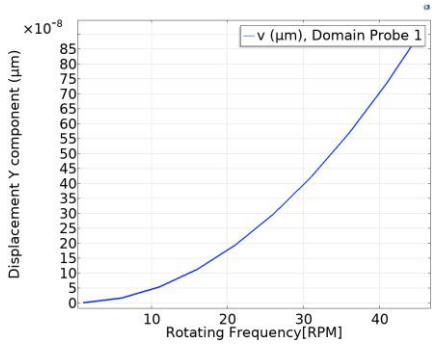

Fig 5: Graphical representation of the displacement achieved.

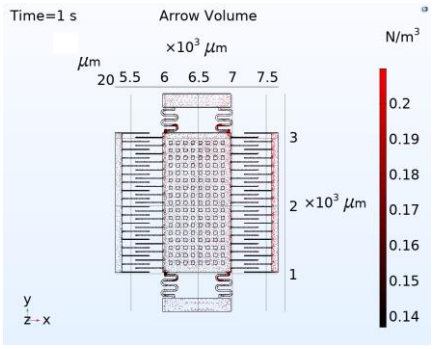

(a)

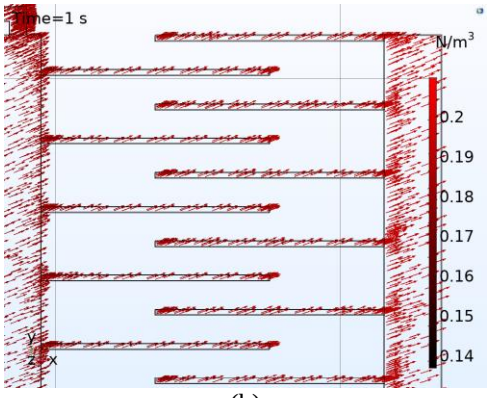

(b)

Fig 6: (a) The direction of the field distribution is shown (b) shows an enlarged image of the same for the comb structures.

In Fig 6 (a) & (b) the different domains of the rotating frame are represented with the volume arrow. In this the arrows represents the direction of the force acting on the structure. The force is applied throughout the structure where volume load and the impact are represented through the volume arrow as the effect of the load in respective of the rotational force applied in the sensor.

IV. Fabrication Feasibility

The steps that can be followed to fabricate the sensor is shown in Fig 7.

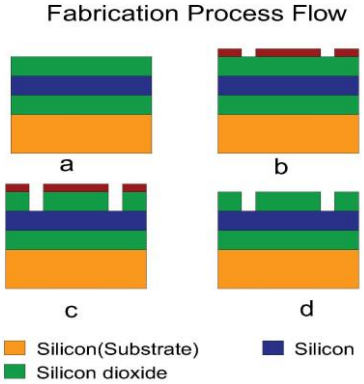

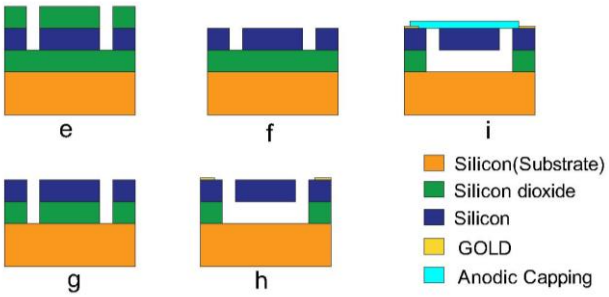

Fig 7: Process flow to fabricate the MEMS device.

Fig 7, shows a SOI wafer with a thermally grown oxide layer. On exposure to UV PPR patterning is done on the oxide layer as shown in b. Using Buffer Oxide Etching, SiO2 patterning is achieved. Then the PPR is stripped off using acetone as shown in d. By DRI etching Silicon is patterned as in e. By DRI etching the SiO2 layer is removed as shown in g. Then the proof mass is released by wet etching as in h. By metal deposition gold is deposited and capping is done by anodic bonding as shown in i.

An external magnetic field is achieved by a pair of magnetic flux concentrators made of a soft magnetic material like NiFe alloy. The flux concentrator is placed along the y axis on either side of the magnetometer. Between 10^{-3}T and 10^{-6}T the suggested magneto-gyro sensor works the best.

V. Conclusion

An integrated system of MEMS-based gyroscope and magnetometer has been designed. The fabrication steps involved are discussed. A resolution of 3 rads/sec has been achieved for the gyroscope. This suggested Magneto-Gyro sensor can account for the lacking sensitivity in the traditional Instrument Landing system making it more efficient and reliable.

References

1. Yazdi, N.; Ayazi, F.; Najafi, K. (1998). Micromachined inertial sensors. , 86(8), 1640–1659
2. W. Geiger, J. Bartholomeyczik, U. Breng. 2008. MEMS IMU for AHRS Applications. Northrop Grumman, Electronic Systems., 1-7.
3. Singh, P.; Gupta, P.; Srivastava, P.; Chaudhary, R. K. (2013). [IEEE 2013 International Conference on Energy Efficient Technologies for Sustainability (ICEETS) - Nagercoil (2013.4.10-2013.4.12)] 2013 International Conference on Energy Efficient Technologies for Sustainability - Design and modeling of MEMS capacitive gyroscope.
4. Wickenden, D.K.; Givens, R.B.; Osiander, R.; Champion, J.L.; Oursler, D.A.; Kistenmacher, T.J. MEMS-based resonating xylophone bar magnetometers. Micromach. Devices Compon **1998**, IV, 350–358.